

Nonlinear Wave Forces on a Rubble Covered Pipeline

William G. McDougal¹
Norimi Mizutani²
Ayman M. Mostafa³

Abstract

A nonlinear numerical model is developed for the interaction of waves with a pipeline covered with rubble. The wave field utilizes a fully nonlinear potential formulation while the porous medium is governed by modified Navier-Stokes equations. The model employs the BEM in the water column and the FEM in the rubble layer. Wave forces on the pipeline are calculated by integrating pressure around the pipeline perimeter. The numerical and experimental results for the wave kinematics in the pipeline vicinity are found to be in reasonable agreement. Numerical analyses indicate that the horizontal wave force is larger than the vertical force for all tested wave and rubble conditions. Forces increase with increasing wave height and decreasing depth. However, for the cases examined there is an intermediate water depth at $h/L \approx 1/6$ for which the forces are largest. The armor stone size and rubble layer porosity have little influence on the magnitudes of the forces. The horizontal force is nearly independent of the depth of rubble cover over the pipeline. However, the vertical force increases significantly as the depth of cover decreases. Also, for partial pipeline cover, the maximum horizontal and vertical forces are more in phase, which combined with the larger vertical force, results in a substantially less stable condition.

¹ Professor, Department of Civil Engineering, Oregon State University, OR 97331, USA

² Associate Professor, Department of Civil Engineering, Nagoya University, Nagoya 464-8603, Japan

³ Assistant Professor, Department of Civil Engineering, Nagoya University, Nagoya 464-8603, Japan

Background

Marine pipelines in nearshore water are often either buried or covered with an armor layer. This reduces the wave forces on the pipeline and the possibility of seabed scour around the pipeline. This may also protect the pipeline from mechanical damage due to anchor drag or fishing nets. In the case of armor protection, little design information is available for estimating the magnitude of wave forces on the pipeline. As a result, designs for large projects are often verified with physical models. During the past few years, several such model studies have been conducted at the O.H. Hinsdale Wave Research Laboratory at Oregon State University. Typical conditions are shown in Figure 1. These pipelines are all outfalls with pipe diameters that range from 1.1m to 3.7m. The protective armor stone diameter ranges from 0.4m to 1.1m. These conditions are representative of outfall conditions on the west coast of the United States. In the physical model tests, typical design concerns include the following: Is the armor stone stable? What is the minimum stable cross-section for the armor? If the pipeline loses weight due to air or gas in the line, is the ballast sufficient to maintain stability? Will the flow around the pipeline and armor induce seabed scour? The objective of the present study is to develop a numerical model to begin to address these issues. At this point in the model development, the intent is not to replace physical model testing, but rather to narrow the range of conditions tested in the laboratory to the most promising alternatives. The numerical model can also be used to provide fast results prior to the experiment at low cost.

The proposed model is a direct extension of previous work by the authors. Mizutani, et al. (1996) developed a coupled BEM-FEM model to study the nonlinear interaction between waves and a submerged breakwater. This model was successful in predicting 2-D wave transformations over a submerged breakwater. Next, Mizutani, et al. (1998) developed a coupled BEM-FEM model for wave, submerged breakwater, and seabed nonlinear interaction. This model incorporated the seabed and the porewater flow. The validity of the BEM-FEM model was demonstrated in comparisons with experimental measurements for a submerged breakwater on a sand seabed. This progression of model development lends itself well to the inclusion of a pipeline within the rubble structure. The objectives of the paper are to develop a numerical model for wave-rubble interaction and wave forces on a marine pipeline.

Figure 2 shows different armor configurations. The pipeline may be wholly buried within the armor layer, partially exposed or heavily exposed. All three are used in practice. The fully covered alternative provides greater protection and stability, but is also more costly. How much the armor section can be reduced is a major consideration in the design. Figure 3 shows nomenclature used to describe the geometry of the armor protection.

Numerical Formulation

The model domain is shown in Figure 4. The free surface is S_f , the mudline along the bottom is S_B , the surface of the armor is S_s , and the pipe surface is S_C . In the water column, the fluid is assumed to be inviscid and incompressible and the flow is irrotational. This leads to a formulation based on a velocity potential. Since this is a potential flow formulation, vortex shedding or other dissipation mechanisms are not included in the water column. The governing equations for the wave field are conservation of mass (Laplace Equation) with pressure recovered from the energy equation. The flow in the porous rubble is modeled by conservation of mass and momentum. The porewater is assumed to be viscous and incompressible and the resistance terms in the momentum equation are based on the Forchheimer equation.

Wave Field:

Governing equation:

$$\frac{\partial^2 \phi}{\partial X^2} + \frac{\partial^2 \phi}{\partial Z^2} = q, \quad q(X, Z, t) = U_o(Z, t)\delta X \tag{1}$$

Boundary Conditions:

$$\frac{\partial \phi}{\partial n} = n_z \frac{\partial \phi}{\partial z} \tag{2} \quad (\text{on } S_f)$$

$$\frac{\partial \phi}{\partial n} = 0 \tag{3} \quad (\text{on } S_B)$$

$$\frac{\partial \phi}{\partial n} = V_n \tag{4} \quad (\text{on } S_s)$$

$$\frac{\partial \phi}{\partial n} + \frac{1}{2}(\nabla \phi)^2 + g\eta + \mu\phi - \int_{x_1}^x \frac{\partial \mu}{\partial X} \phi dX = 0 \tag{5} \quad (\text{on } S_f)$$

$$\frac{\partial \phi}{\partial X} = \frac{1}{\sqrt{gh}} \left(\frac{\partial \phi}{\partial t} + \mu\phi + \int_{x_2}^{x_1} \frac{\partial \mu}{\partial X} \phi dX \right) \tag{6} \quad (\text{on } S_L)$$

$$\frac{\partial \phi}{\partial X} = -\frac{1}{\sqrt{gh}} \left(\frac{\partial \phi}{\partial t} + \mu\phi - \int_{x_3}^{x_4} \frac{\partial \mu}{\partial X} \phi dX \right) \tag{7} \quad (\text{on } S_R)$$

$$\mu_{\max} = (0.25 \sim 0.50) \sqrt{\frac{g}{h}} \tag{8}$$

in which ϕ = velocity potential, η = water surface elevation wrt SWL, n_z = outward normal with respect to the Z axis, V_n = velocity component normal to the boundary, μ = damping factor, h = still water depth, X, Z = horizontal and vertical coordinates, and t = time. An idealized wave tank similar to that of Ohyama and Nadaoka (1991) is adapted to simulate the nonlinear deformations over a marine pipeline.

The numerical solution technique used for the wave field is the boundary element method (BEM). The BEM formulation maps the 2-D problem onto the 1-D boundary. The boundary is discretized using linear elements at a spacing of approximately 20 elements per wave length in the horizontal and 8 elements along the vertical boundaries at the ends of the domain. Typically about 150 boundary elements were employed.

Porous Flow:

Governing equations:

$$\frac{\partial U}{\partial X} + \frac{\partial W}{\partial Z} = 0 \quad (9)$$

$$A \frac{\partial U}{\partial t} + B(U \frac{\partial U}{\partial X} + W \frac{\partial U}{\partial Z}) + C \frac{\partial P}{\partial X} + EU + FU \sqrt{U^2 + W^2} = 0 \quad (10)$$

$$A \frac{\partial W}{\partial t} + B(U \frac{\partial W}{\partial X} + W \frac{\partial W}{\partial Z}) + C \frac{\partial P}{\partial Z} + EW + FW \sqrt{U^2 + W^2} = 0 \quad (11)$$

$$A = \left(1 + \frac{1-\varepsilon}{\varepsilon} C_a \right) / \varepsilon g, \quad B = 1 / \varepsilon^2 g, \quad C = 1 / \gamma, \quad E = \frac{6(1-\varepsilon)\nu C_{D2}}{g \varepsilon^2 D^2}$$

$$F = \frac{C_{D1}(1-\varepsilon)}{2gD\varepsilon^3}, \quad P = p - \gamma Z \quad (\text{Mizutani et al., 1996})$$

Boundary conditions:

$$P = -\rho \frac{\partial \phi}{\partial t} - \frac{\rho}{2} \left\{ \left(\frac{V_n}{\varepsilon} \right)^2 + V_s^2 \right\} - \gamma Z \quad (\text{on } S_S) \quad (12)$$

$$V_n = W \cos \theta \pm U \sin \theta \quad (\text{on } S_S) \quad (13)$$

$$V_s = \frac{\partial \phi}{\partial S} \quad (\text{on } S_S) \quad (14)$$

$$V_n = 0 \quad (\text{on } S_C) \quad (15)$$

in which U , W = horizontal and vertical seepage velocities, P = total pressure, p = dynamic pore pressure, ε = porosity, C_a = added mass coefficient, g = acceleration of gravity, ν = kinematic viscosity of water, γ = unit weight of water, D = stone diameter, θ = side slope angle, C_{D1} , C_{D2} = drag coefficients, and A , B , C , D , E , F are notational constants.

The rubble flow model is solved using the finite element method (FEM). Since there are internal variations in the flow properties and dissipation, the rubble problem does not conveniently map to a boundary and must be solved in 2-D. The fundamental unknowns are U , W , and P . These are approximated using isoparametric finite elements. The flow in the rubble includes nonlinear dissipation through the Forchheimer resistance terms.

On the surface of the pipeline, the normal component of velocity is zero. The forces are calculated by integrating the pressure around the pipeline. The force does not include drag. As a result, the solution is most appropriate for large diameter pipelines in which the forces are diffraction dominated. On the surface of the rubble, the pressure and normal fluid flux from the BEM and FEM solutions are required to match. This matching couples the two solution domains. This leads to a large matrix in which the upper left corner is densely populated (the BEM part), the lower right part is sparsely populated (the FEM part) and the off diagonal corners are zero. The form of this matrix allows the use of efficient matrix algorithms. The equations are integrated in time by explicit finite difference. The time step varies from $T/24$ to $T/144$ depending upon the degree of nonlinearity in the problem.

This formulation is well suited for the present application. It is reasonably efficient, but includes nonlinear terms at the free surface and in the rubble matrix. The formulation is less suitable for breaking waves, but the application of the model is intended for pipelines outside of the surf zone where breaking is less significant. The model can also be modified to include the influence of wave angle. In this paper, only waves which have crests parallel to the pipeline are considered. In practice, there are many cases where the wave crests are nearly perpendicular to the pipeline.

Physical Model Tests

Several pipeline stability tests have been conducted at the Oregon State University Wave Research Laboratory. Tests were conducted in the large wave flume which is 104m long, 3.7m wide, and 4.6m wide. Simple periodic, random, nonbreaking, and breaking wave conditions have been examined. The model is typically placed near the center of the flume at an orientation to simulate the prototype conditions. Figure 2 gave examples of three tested configurations. Incident and reflected waves are determined using a Goda wave gage array. The transmitted wave height and fluid velocities in the vicinity of the structure are also measured. The stability of the armor is monitored with underwater video. A variety of parameters are varied including the wave conditions, stone size, rubble geometry, and buoyancy of the pipeline.

Table 1 gives several predicted and measured results for the horizontal velocity. Laboratory results are for an 11.4 cm diameter pipe in 158 cm of water armored with 2cm stone. Two wave height conditions are given which differ by approximately a factor of 2; 25.3cm and 54.3cm. Figure 5 shows numerical model results for the horizontal velocity computed for these conditions. These two cases span a range from nearly linear to nonlinear wave conditions. In general, the agreement is reasonable; but as indicated by these examples, the variation can be as much as 30%.

Table 1 Measured and computed horizontal velocities near a rubble covered pipeline.

	Run A180101 $H=25.3\text{cm}$, $T=3.65\text{s}$, $h=158\text{cm}$		Run A1830209 $H=54.3\text{cm}$, $T=4.95\text{s}$, $h=158\text{cm}$	
	Numerical	Measured	Numerical	Measured
U_{max} (cm/s) Offshore	28.0	28.5	109.5	83.2
U_{min} (cm/s) Offshore	-26.0	-25.4	-57.9	-51.8
U_{max} (cm/s) Above pipe	30.0	25.3	65.8	65.2
U_{min} (cm/s) Above pipe	-29.0	-21.3	-36.5	-35.4

Results

Figure 6 shows the horizontal and vertical forces for a fully buried pipeline and a partially exposed pipeline. The gap at the beginning of the runs is the time required for the waves to propagate from the generation boundary to the pipeline. Results are shown for time durations of 6 and 8 wave periods. The numerical computations remained stable beyond this time. The horizontal force is much less

than the vertical force and is approximately 90° out of phase for the fully buried case. For the partially exposed case, the horizontal force has increased slightly, but the vertical force has increased significantly. The phase difference between the two forces is approximately 60° . For the partially exposed case, there is an increase in the magnitude of the vertical force and the maximum horizontal and vertical forces are closer in phase. As a result, the partially exposed pipeline is much less stable.

Figure 7 shows the pressure field in the rubble around the pipeline and Figure 8 shows the porewater velocity. At this phase, the pressure gradient drives a flow in the direction of wave propagation. The resulting flow is accelerated around the pipeline and may be constricted beneath the pipeline if the clearance above the seabed is small.

The numerical model provides an opportunity to efficiently determine the sensitivity of the pipeline force to wave and rubble conditions. The base conditions for this sensitivity analysis are given in Table 2. First the wave height, period, and depth are considered. Figure 9 shows the dimensionless horizontal and vertical forces on the pipeline as a function of the wave height. The forces are scaled by the weight density of the water, the wave height, and the pipeline diameter. It is seen that this linear scaling captures the wave height dependency over a range of conditions. Figure 10 shows the influence of the wave period on the pipeline forces. There is an intermediate period for which the forces are a maximum. This period corresponds to a dimensionless water depth of $h/L \approx 1/6$ for this particular rubble geometry. The figure shows both the positive and negative forces. The horizontal forces are generally larger in the direction of wave propagation and this difference increases as the waves become more nonlinear. The upward vertical forces are larger than the downward forces. The influence of the water depth is shown in Figure 11 and is as anticipated, the deeper the water, the smaller the forces. The horizontal forces scale as approximately $1/h$ for these shallow to intermediate depth conditions.

Three rubble parameters are examined, the porosity of the rubble matrix, the stone diameter, and the depth of burial of the pipeline. Porosities from $\varepsilon = 0.24$ to 0.40 were examined and found to have little influence on the magnitude of the forces. The stone diameter also has very little influence on the forces on the pipeline. The influence of depth of burial is shown in Figure 12. The results indicate that the horizontal force is not strongly influenced by the depth of cover. The vertical force increases as the depth of cover decreases. The case with the center of the pipe at the top of the armor ($s/D_p = 0$) corresponds to half of the pipe being exposed. For this case the vertical force is much larger; nearly as large as the horizontal force. It was noted in Figure 6 that the phase of the maximum vertical force is closer to the maximum horizontal force which leads to a larger total force. The numerical model does not include friction or dissipation in the water

Table 2 Base conditions for sensitivity analysis.

H	1.0m
T	9.0s
h	8.0m
D_p	1.0m
D	0.25m
s	1.0m
ε	0.4
B	3.0m

column and these results may be suspect. However, the calculated value is in agreement with the trend of the covered pipeline cases.

Figure 13 shows the influence of the pipe diameter. The dimensionless horizontal force increases nearly linearly with the pipe diameter. Since the forces are calculated based on diffraction theory, this is an anticipated result. The vertical force also increases slightly with the pipeline diameter.

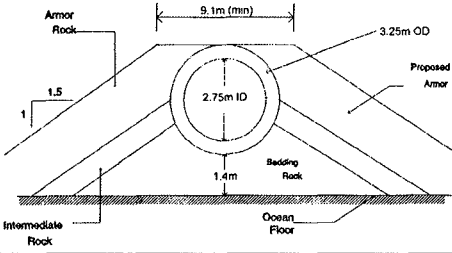
Conclusions

A nonlinear numerical model using BEM in the water column and FEM in the porous rubble has been developed. The numerical model results compared reasonably well with model test results and can adequately simulate the nonlinear interaction between waves and a pipeline covered with rubble protection. It was observed that the horizontal wave force is larger than the vertical force for all wave conditions and rubble configurations examined in this paper. The dimensionless wave forces on a buried pipeline generally decrease as the depth increases. However, there is a wave period dependency that yields a maximum wave force corresponding to $h/L \approx 1/6$. The armor stone size and armor layer porosity have little influence on the magnitudes of the forces. The depth of pipeline burial has little influence on the magnitude of the horizontal force. However, the vertical force on a partially exposed pipeline is much larger than for a fully covered pipeline and is closer to being in phase with the horizontal force. As a result, the partially buried case is much less stable.

References

- Bailey, S.B. (1992) *Goleta Sewer Outfall Stability Tests*, Masters of Science Project, Ocean Engineering Program, Civil Engineering Department, Oregon State University, Corvallis, OR, 138 pp.
- Freeman, P. (1994) *South Bay Tunnel Outfall Stability Tests*, Masters of Science Project, Ocean Engineering Program, Civil Engineering Department, Oregon State University, Corvallis, OR, 177 pp.
- Mizutani, M., W.G. McDougal, and A.M. Mostafa (1996) BEM-FEM analysis of nonlinear interaction between wave and submerged breakwater, *Proceedings of ICCE*, Orlando, Florida, 2377-2390.
- Ohyama, T. and K. Nadaoka (1991) Development of a numerical wave tank for analysis of non-linear and irregular wave field, *Fluid Dynamics Research*, 8:231-251.
- Mizutani, N., A. Mostafa and K. Iwata (1998) Nonlinear regular wave, submerged breakwater and seabed dynamic interaction, *Coastal Engineering*, 33:177-202.

Ruggiero, P. (1993) *Point Loma Sewer Outfall Stability Tests*, Masters of Science Project, Ocean Engineering Program, Civil Engineering Department, Oregon State University, Corvallis, OR, 177 pp.



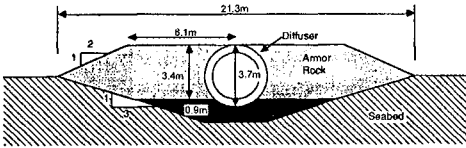
Point Loma Outfall

$H = 8.5\text{m}$, $h = 70\text{m}$

$L_p = 3,350\text{m}$, $D_p = 3.25\text{m}$

$D = 1.1\text{m}$

(after Ruggiero, 1993)



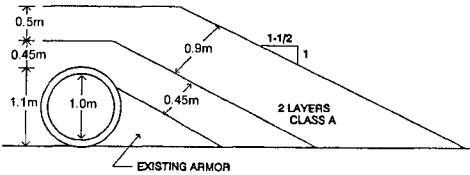
South Bay Tunnel Outfall

$H = 18.4\text{m}$, $h = 28\text{m}$

$L_p = 6,100\text{m}$, $D_p = 3.7\text{m}$

$D = 0.7\text{m}$

(after Freeman, 1994)



Goleta Outfall

$H = 3.7\text{m}$, $h = 26\text{m}$

$L_p = 1,770\text{m}$, $D_p = 1.1\text{m}$

$D = 0.39\text{m}$

(after Bailey, 1992)

Figure 1 Examples of pipeline stability tests.

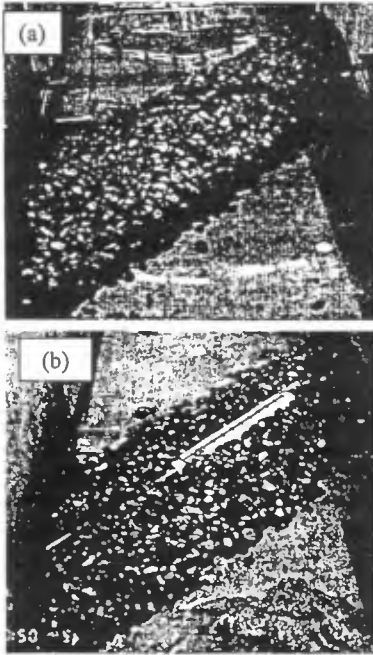


Figure 2 Examples of (a) fully covered, (b) partially covered, and (c) fully exposed pipelines.

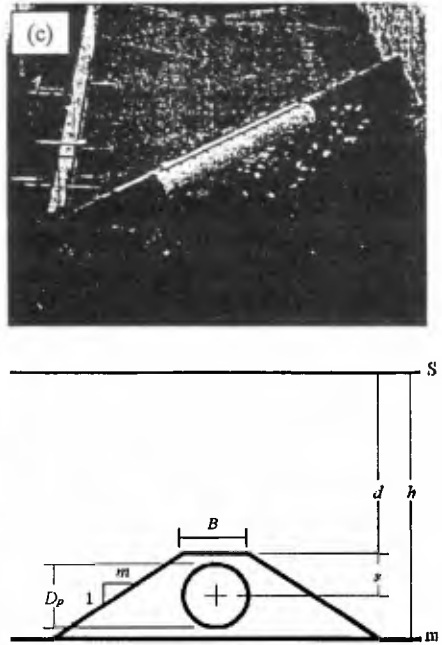


Figure 3 Definition sketch.

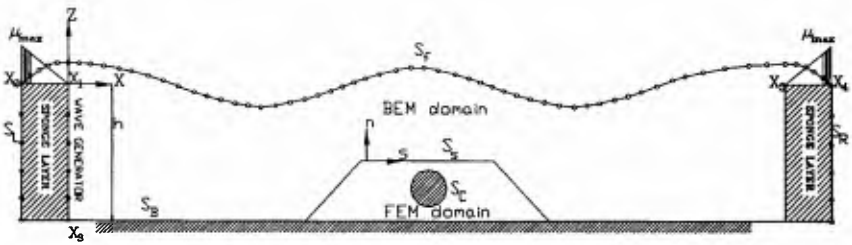


Figure 4 Model domain.

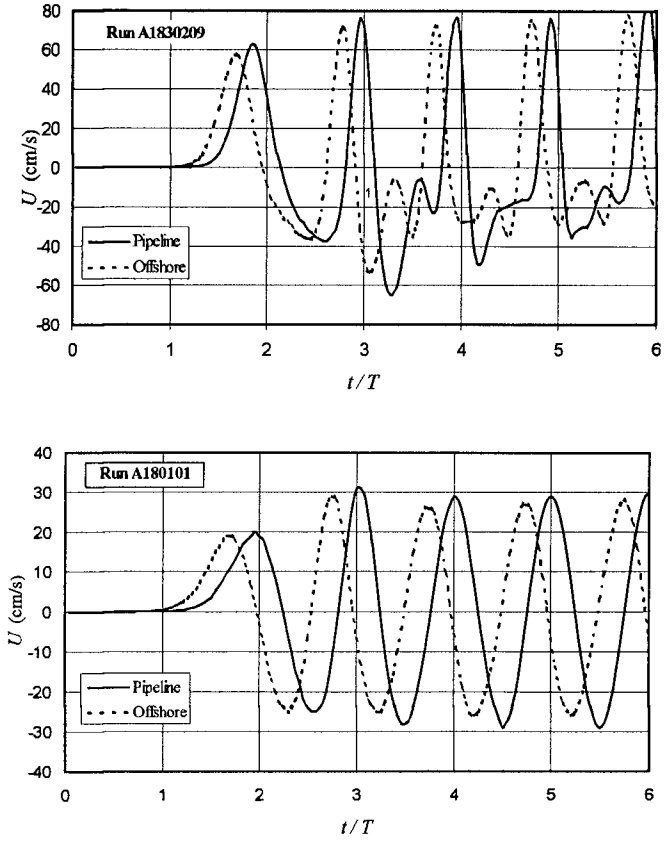


Figure 5 Computed horizontal velocities for two physical model cases.

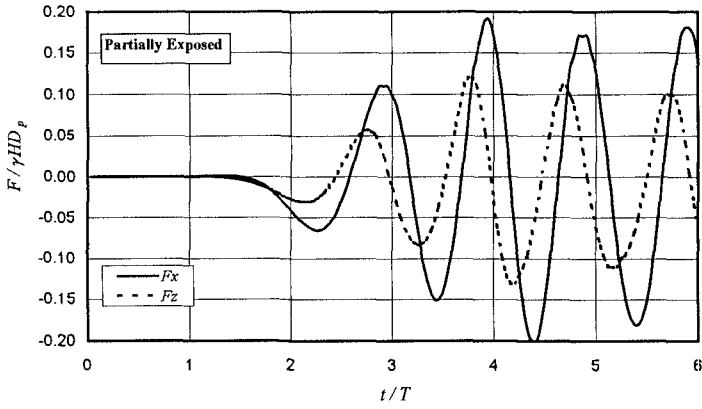
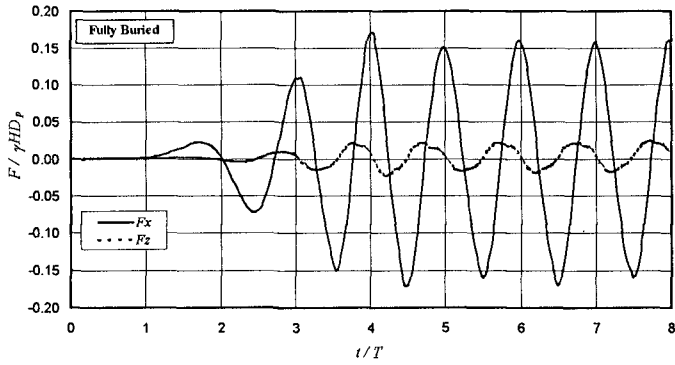


Figure 6 Time history of wave forces acting a fully buried and a partially exposed pipeline.

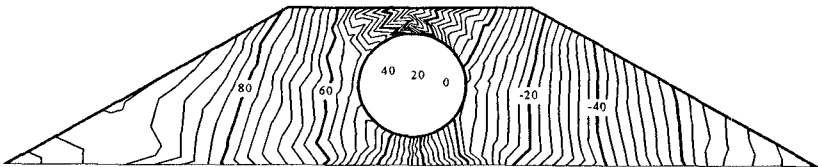


Figure 7 Pore pressure around a fully buried pipeline at $t/T=6.0$.

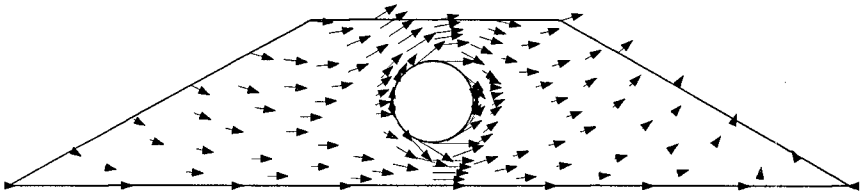


Figure 8 Porewater velocity around a fully buried pipeline at $t/T=6.0$.

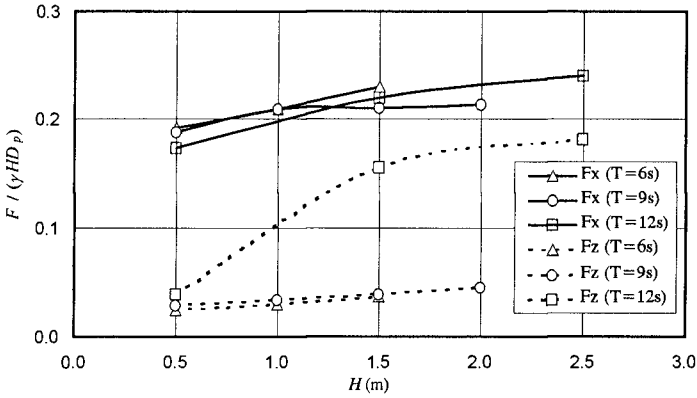


Figure 9 Influence of wave height on dimensionless force.

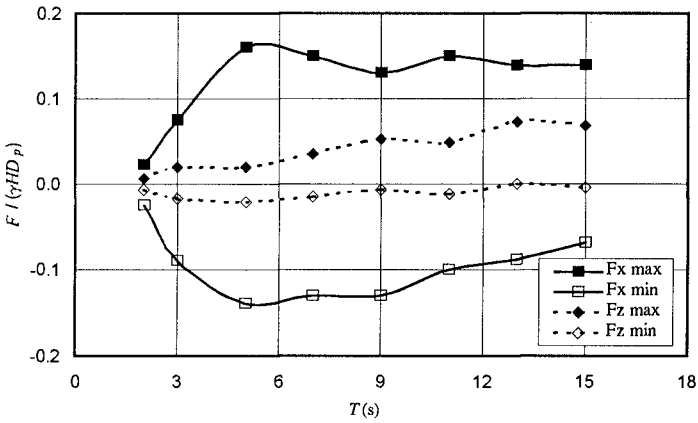


Figure 10 Influence of wave period on dimensionless force.

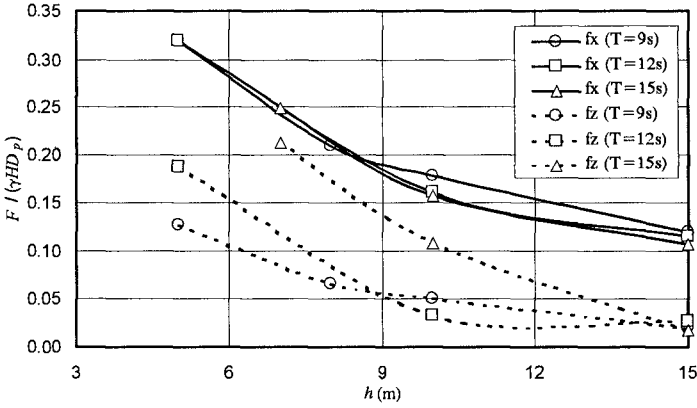


Figure 11 Influence of water depth on dimensionless force.

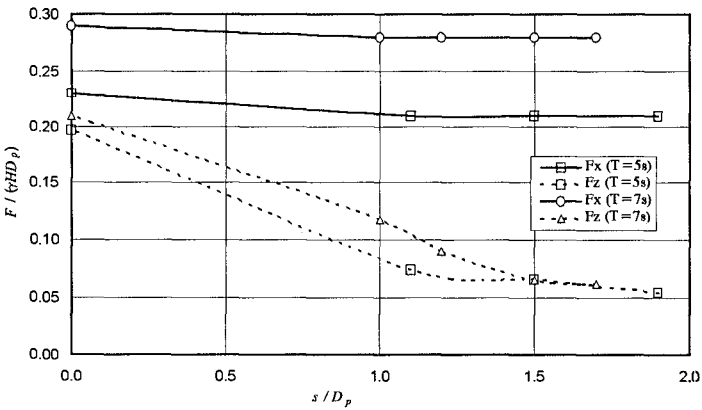


Figure 12 Influence of burial depth on dimensionless force.

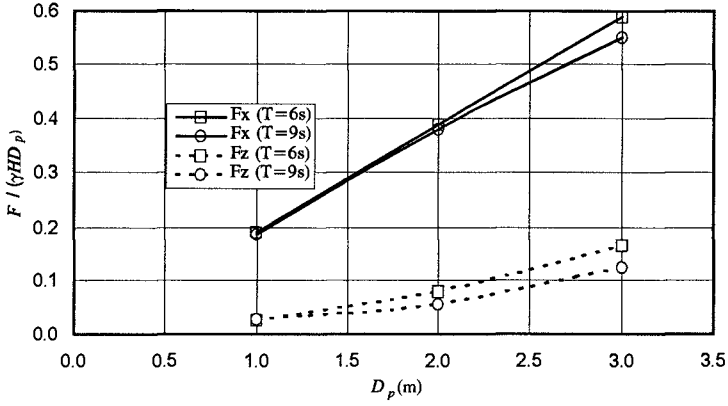


Figure 13 Influence of pipe diameter on dimensionless force.